A Frequency-Dependent Scalar Magneto-Elastic Hysteresis Model Derived Using Multi-Scale and Jiles–Atherton Approaches

B. Sai Ram[1], A. P. S. Baghel[1,2,3], S. V. Kulkarni[1], *Fellow, IEEE*, L. Daniel[2], and I. C. Nlebedim[3]

[1]Department of Electrical Engineering, IIT Bombay, Mumbai 400076, India
[2]Group of Electrical Engineering-Paris (GeePs), UMR CNRS 8507, CentraleSupélec, Univ Paris-Sud, Université Paris-Saclay, Sorbonne Université, 91192 Gif-sur-Yvette, France
[3]Critical Materials Institute, The Ames Laboratory, US DOE, Ames, IA 50011 USA

The effects of mechanical stress on static and dynamic (frequency-dependence) magnetic behaviors of soft magnetic materials have to be modeled. A scalar static magneto-elastic hysteresis model is proposed which combines a simplified version of a multi-scale approach and the Jiles–Atherton (JA) model. The magneto-elastic hysteresis model is extended to include dynamic losses using the field separation approach. The effect of stress on dynamic loss components, particularly on the excess loss, is approximated using an exponential function. The model is validated with measured dynamic hysteresis loops over a frequency range of up to 1 kHz and uniaxial mechanical loading up to 50 MPa (both compressive and tensile stresses). The proposed model still preserves its simplicity and inverse form representation, which makes it quite amenable to numerical implementations. The approach can be applied to model magneto-elastic effects in the elastic range.

Index Terms— **Electrical steel, iron loss, Jiles–Atherton (JA) model, magneto-elasticity, magnetostriction, multi-scale (MS) model.**

I. Introduction

THE need for efficient use of energy materials is critical for high-performance electrical machines and also drives the desire for low weight and compact systems. However, such systems (e.g., high-speed motors) frequently experience high levels of mechanical stresses [1]. Other sources of induced mechanical stresses are temperature gradients, manufacturing processes (e.g., cutting and stamping), and assembly processes (e.g., shrink-fitting) [1]–[3]. These stresses affect the magnetic properties (permeability and losses) of the core laminations in electrical machines [2]. Therefore, an accurate model is required to account for magneto-mechanical properties [1], [2], [4]–[9] in order to precisely compute losses.

A proper understanding of the magneto-elastic effects is required to derive an accurate model. Magnetization under the influence of stress includes the following main mechanisms [10]: 1) movement of domain walls due to pressure on 90° domain walls; 2) variation in energies of pinning sites; and 3) irreversible changes in the domain structure. It was concluded in [11] that domain wall motion alone cannot explain the effect of the stress because of the change of various microstructure parameters in complex manners. The stress effects on the magnetization process of soft magnetic materials can be experimentally observed from the change in shape and area of hysteresis loops. Also, it has been observed, particularly in non-oriented (NO) steels under compressive stress, that hysteresis loops exhibit local widening known as "kink" and all of the loops pass through two points called coincident points (C_1 and C_2) as shown in Fig. 1(a) and they can be correlated with Villari reversal [12]. It should be noted that hysteresis loops in Fig. 1 are measured using the setup described in Section II. In [13], Brown and Bozorth stress fields were used to model this phenomenon. The stress effects on the magnetic properties of NO materials are analyzed using the observation of magnetic domains in a recent work [14]. The observed effect of the compressive stress can be explained as it disfavors the magnetic easy axis along the rolling direction. However, tensile stress first improves the magnetic properties up to a certain value of the applied stress and then starts to deteriorate magnetic properties [15].

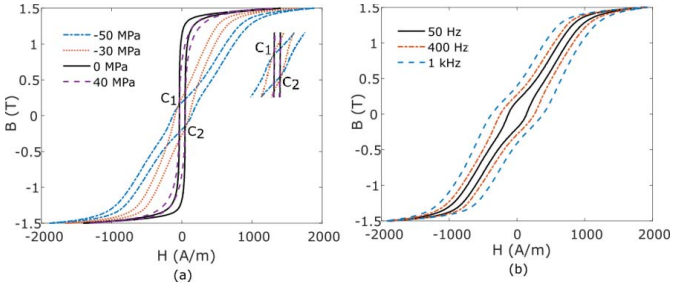

Fig. 1. (a) Effect of tensile stress (positive values) and compressive stress (negative values) on the measured hysteresis loops of NO materials. (b) Frequency-dependent loops at a compressive stress of 50 MPa.

Various modeling approaches are available to formulate the magneto-elastic behavior of iron-silicon steels [6], [7], [16], [17]. Most of the available magneto-elastic models in the literature are extensions of classical models [6] like the Jiles–Atherton (JA) (using an effective field) [16] and Preisach models (using a distribution function) [17]. These models are usually restricted to isotropic materials and uniaxial stress

Manuscript received August 19, 2019; revised October 6, 2019; accepted October 24, 2019. Date of publication January 10, 2020; date of current version February 19, 2020. Corresponding author: B. Sai Ram (e-mail: sairam.eng10@gmail.com).

Color versions of one or more of the figures in this article are available online at http://ieeexplore.ieee.org.

Digital Object Identifier 10.1109/TMAG.2019.2950751

configurations. Another approach based on energy equilibrium known as the multi-scale (MS) model is developed, particularly to formulate the magneto-elastic characteristics [7]. The model is extended to consider the hysteresis effects using Kádár product [18] and Hauser approaches [19]. However, an extension of the above-mentioned approaches to consider dynamic or frequency-dependent behavior is not available in the literature.

According to the statistical loss theory, iron losses can be separated into static hysteresis loss, classical eddy current loss, and excess loss [20]. The inclusion of dynamic losses results in horizontal widening of hysteresis loops as evident from Fig. 1(b). Numerous attempts are reported on the description of stress effects on the core loss components using the loss separation approach [4], [21].

In this article, an anhysteretic function formulated using the MS approach [22] is used in its scalar form to consider uniaxial stress whose direction is along the applied magnetic field (H). Hysteretic effects are included using the JA model. Stress effects on the pinning constants are modeled using a Gaussian function in order to simulate the kink [18], [23]. In this article, the field separation approach is used to include dynamic losses [24]. The stress effects on the excess loss component are formulated in the model via its coefficient. The proposed dynamic magneto-elastic model is used to predict hysteresis losses up to the 1 kHz frequency range and uniaxial mechanical stress up to 50 MPa (both compressive and tensile stresses) in a finite element method (FEM) simulation of a single sheet tester (SST). The model is validated with the measured hysteresis loops and losses.

II. Proposed Hybrid Approach

Frequency-dependent (up to 1 kHz) hysteresis loops with pure sinusoidal-flux density (B) of 1.5 T were measured under both compressive and tensile stresses (0–50 MPa) for a sample of NO material (M235-35A) using an SST (BROCKHAUS-MPG 200 D) device. The device contains pneumatic tension and compression units in order to apply mechanical loadings [4], [5].

A. Derivation of Anhysteretic Magnetization

An analytical magneto-elastic anhysteretic magnetization is derived using the MS approach in [22] for multi-axial stress conditions and unidirectional magnetic-field excitation

$$M_{\text{an}} = M_{\text{s}} \frac{A_x \sinh(\kappa H)}{A_x \cosh(\kappa H) + A_y + A_z}. \tag{1}$$

Here, $\kappa = \mu_0 A_{\text{s}} M_{\text{s}}$, $\alpha_{\text{s}} = 1.5\ A_{\text{s}} \lambda_{\text{s}}$, $A_{\text{s}} = 1/(\mu_0 a M_{\text{s}})$, $a = M_{\text{s}}/3\chi_o$, and $A_i = e^{\alpha_{\text{s}} \sigma_{ii}}$, $i = x, y,$ and z. σ_{ii} is the applied stress along an iith direction, M_{s} is the saturation magnetization, A_{s} is a material parameter related to initial susceptibility, and λ_{s} is the saturation magnetostriction constant. Model (1) is basically developed for a multiaxial case. It should be noted that in the multiaxial case, the stress is a tensor (a 3×3 matrix in 3-D case), and thus, (1) can be applied to model stress in 3-D.

B. Development of the Hybrid Magneto-Elastic Hysteresis Model for Uniaxial Stress

In this article, (1) is simplified for uniaxial stress conditions with the stress being applied along the direction of the magnetic field. This results in $A_y = A_z = 0$ and reduces the definition of stress into a scalar form. The magnetic field is modified to an effective magnetic field H_e ($=H + \alpha M$) to consider domain formation using the mean-field theory. The modified scalar magneto-elastic anhysteretic magnetization for uniaxial stress is

$$M_{\text{an}} = M_{\text{s}} \frac{A \sinh(\kappa H_e)}{A \cosh(\kappa H_e) + 2}, \quad A = e^{\alpha_{\text{s}} \sigma}. \tag{2}$$

The hysteresis behavior is simulated using the scalar JA model, and its inverse form can be written as

$$\begin{aligned} \frac{dM}{dB} &= \left[\frac{(1-c)\frac{dM_{\text{irr}}}{dB_e} + \frac{c}{\mu_0}\frac{dM_{\text{an}}}{dH_e}}{1 + c(1-\alpha)\frac{dM_{\text{an}}}{dH_e} + \mu_0(1-c)(1-\alpha)\frac{dM_{\text{irr}}}{dB_e}} \right] \\ k &= k_0(e^{\beta_h \sigma}) \left(1 + e^{-\frac{(B-\delta B_c)^2}{b}}\right) \\ \frac{dM_{\text{irr}}}{dB_e} &= \frac{M_{\text{an}} - M_{\text{irr}}}{\mu_0 k \delta}, \quad M_{\text{irr}} = \frac{M - cM_{\text{an}}}{1-c}. \end{aligned} \tag{3}$$

Here, μ_0 is the permeability of free space, M_{irr} is the irreversible magnetization, δ is the directional parameter which is equal to -1 for $dB/dt < 0$ and $+1$ for $dB/dt > 0$, k is the pinning parameter which simulates kinks using a Gaussian function, and B_c (0.2 T, in this analysis) is the magnitude of magnetic-flux density at coincident points. As shown in Fig. 1(a), the kink is a localized widening of the hysteresis loop and it can be described by using Villari reversal (a reciprocal effect) [12], which explains that the value of induction for an applied magnetic field in the low field region increases with stress and then decreases for higher induction levels. The proposed model can also be extended to consider multiaxial stress by using the equivalent stress concept proposed in [25].

C. Inclusion of Stress-Dependent Dynamic Losses

The field separation approach [24], which is represented by (4), is used to integrate dynamic losses in the proposed analysis

$$H_{\text{total}} = H_{\text{hys}} + H_{\text{ec}} + H_{\text{ex}}. \tag{4}$$

Here, H_{total}, H_{hys}, H_{ec}, and H_{ex} are total magnetic field, static hysteresis field, classical eddy current field, and excess loss field, respectively. The classical loss component depends on thickness and conductivity, but it is independent of the domain structure of the material [21]. Therefore, it is assumed as independent of mechanical stresses and can be represented as

$$H_{\text{ec}} = k_{\text{ec}} \frac{dB}{dt}, \quad k_{\text{ec}} = \frac{d^2}{12\rho}. \tag{5}$$

Here, d and ρ are thickness and resistivity of laminations. The excess loss depends on domain configurations of the material and so on the mechanical stress [21]. It can be modeled using an exponential function as

$$H_{\text{exc}} = k_{\text{ex}} \left| \frac{dB}{dt} \right|^{1/2}, \quad k_{\text{ex}} = k_{\text{ex0}} e^{\beta_{\text{ex}} \sigma}. \tag{6}$$

TABLE I
MODEL PARAMETERS

	M_s (A/m)	a (A/m)	α	k_o (A/m)	c	b (T^2)	β_h (Pa^{-1})	k_{ex0} $(A/\Omega)^{1/2}$	β_{ex} (Pa^{-1})
Compressive	$1.19e^5$	310	$5e^{-4}$	40	0.2	0.1	0.02	0.02	0.043
Tensile	$1.19e^5$	310	$5e^{-4}$	40	0.2	$15e^{-14}$	$3e^{-4}$	0.02	$1.2e^{-11}$

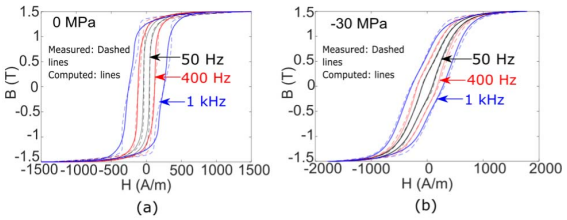

Fig. 2. Comparison of measured (dashed lines) and fit (solid line) under the stress level of (a) 0 MPa and (b) −30 MPa (compressive).

Here, k_{ex0} is the excess loss coefficient for $\sigma = 0$, which can be determined by using the loss separation approach at zero stress condition. β_{ex} is a parameter that can be determined by using k_{ex} for $\sigma = \pm 30$ MPa (computed using the loss separation approach). This exponential function describes the effect of stress on microstructural parameters such as grain size, crystallographic texture, etc., which, in turn, affects the excess loss [21]. As discussed, the classical eddy current loss component is independent of stress, so the parameter k_{ec} (=0.022) can be calculated from its expression in (5). The mechanical stress affects the excess loss component and its dependence is introduced in its coefficient (k_{ex}). Hence, at each stress level, hysteresis data for two different frequencies (here, 50 Hz and 1 kHz) are required to determine the dynamic loss parameters.

The parameters of the anhysteretic function (2) and the JA model (3) are determined at 0 and −30 MPa using an optimization algorithm given in [26]. Stress-dependent k parameter is modeled using the measured loops at 0 and −30 MPa for compressive stress and 0 and 30 MPa for tensile stress. Thus, the parameter identification process requires hysteresis data at two stress levels and two different frequencies. Table I lists the optimized parameters, and the comparison of the fit loops with the measured ones is shown in Fig. 2.

These parameters are then used to model hysteresis loops at various frequencies and stress levels. The comparison of computed loops with measured ones is shown in Fig. 3. By comparing Fig. 3(a) and (b), it is easily seen that the effect of compressive stress [Fig. 3(a)] on magnetic properties is greater compared to that of the tensile stress [Fig. 3(b)], as others have also observed [4], [5], [21]. The consequence of this difference is that the values of parameters for the tensile stress are negligible compared to those for the compressive stress. The normalized rms (NRMS) error is computed as

$$\text{NRMS Error} = \frac{1}{H_{\max}} \sqrt{\left(\sum_{i=1}^{n} (H_{\text{mes}} - H_{\text{comp}})^2\right) \Big/ n} \times 100. \tag{7}$$

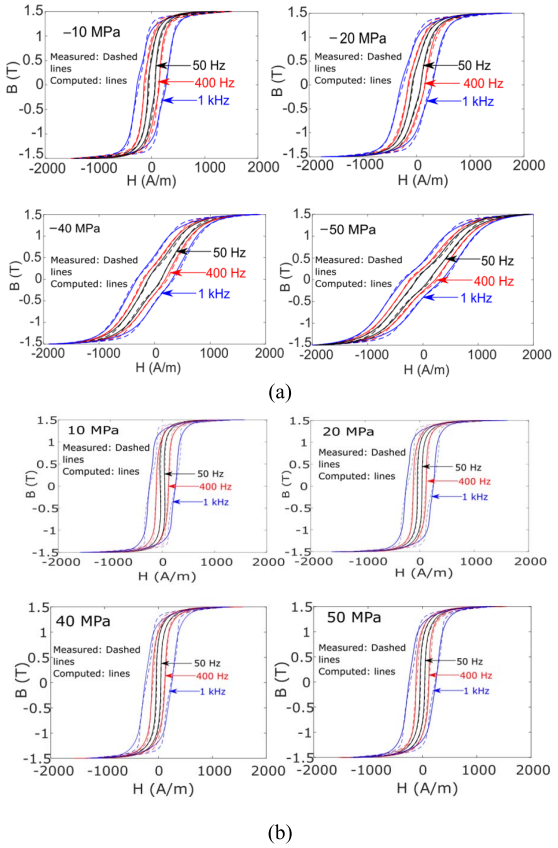

Fig. 3. Comparison of measured (dashed lines) and computed (solid line) at different frequencies for (a) compressive stress and (b) tensile stress.

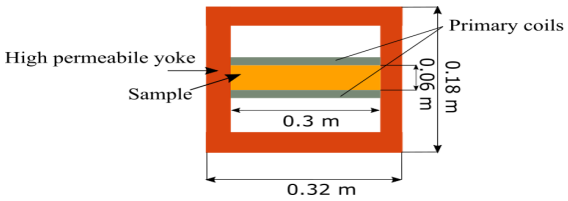

Fig. 4. Geometry of a single sheet tester [5].

Here, n is the number of data points and $H_{\max}$, H_{mes}, and H_{comp} are maximum value, measured data, and computed data of the magnetic field, respectively. The maximum value of NRMS error is 8%, obtained for 10 MPa and 1 kHz.

III. FEM IMPLEMENTATION OF THE PROPOSED MODEL

The proposed dynamic hysteresis model is implemented in the coupled circuit-field FEM simulation of an SST device. A 2-D geometry of the problem is shown in Fig. 4. The number of turns N is 400, and the yoke region is considered lossless with very high permeability. Therefore, the losses are computed at the post-processing stage in the sample region only.

A. Coupled Circuit-Field FEM Formulation

Magnetic-field behavior in the SST is governed by

$$\nabla \times \left(\frac{1}{\mu} \nabla \times \mathbf{A}\right) = J_o = \frac{NI}{S}. \tag{8}$$

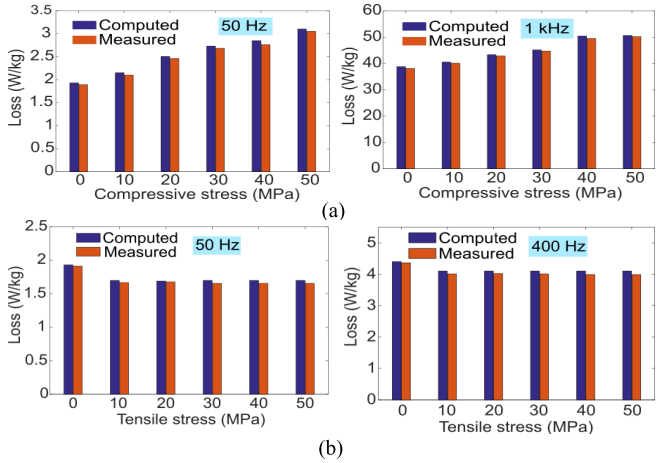

Fig. 5. Comparison of measured and computed losses for (a) compressive stress (b) tensile stress.

Here, S is the coil cross-sectional area and A is the magnetic vector potential. μ is the magnetic permeability, and it is a nonlinear function of induction B and stress σ. The equation to couple the external circuit and the field model is

$$\{U\} = \frac{N}{S}\frac{d}{dt}\left\{\int_S \mathbf{A}\cdot dS\right\} + [R_{\text{ext}}]\{I\} + \frac{d}{dt}[L_{\text{ext}}]\{I\}. \tag{9}$$

Here, U is the applied voltage; I is the current drawn from the source; and R_{ext} and L_{ext} are the circuit resistance and inductance, respectively. After applying the FEM procedure [27], the matrix representation of (8) and (9) is

$$[K][A] + [D][I] = 0 \tag{10}$$

$$[D]'\frac{d}{dt}[A] + [R_{\text{ext}}][I] + [L_{\text{ext}}]\frac{d}{dt}[I] = [U]. \tag{11}$$

In (10), $[K]$ represents the global coefficient matrix and $[D]$ represents the source term. In the local coefficient method (LCM) fixed point method [28], the differential reluctivity can be computed as

$$\nu_{\text{FP}}^{n+1} = C\frac{(H^n - H^{n-1})}{(B^n - B^{n-1})} = C\left(\frac{dH}{dB}\right)^n. \tag{12}$$

Here, C and ν_{FP}^{n+1} are a convergence factor and the fixed point reluctivity at the present time step, respectively. The optimum value of C is chosen as 1.3 for which the simulation is found to converge satisfactorily. At a time step, for all iterations, the value of υ_{FP} is considered as constant. The matrix $[K]$ needs to be computed at each time step, as it is a function of "ν." Equations (10) and (11) are solved by using the Crank–Nicolson method.

B. Results and Discussion

The model is implemented in the FEM simulation of the SST. The number of elements in the problem domain for the simulation is 2688. The CPU time for the execution of the code is 1891 s for an Intel Core i5 processor with 4 GB RAM and allotted memory of 560 MB. Core losses are predicted at 1.5 T for a frequency of up to 1 kHz under different stress levels. Although the skin effect needs to be considered, for the sake of simplicity, it is neglected, while neglecting the skin effect may be thought as a limitation, which is applicable to electrical steel laminations with a thicknesses much less compared to skin depth [27] in which uniform flux distribution can be assumed. A comparison of computed losses measured at different stress levels and frequencies is shown in Fig. 5. The maximum error is 10% for loss prediction, obtained at 0 MPa and 1 kHz. For both compressive and tensile stress cases, each measurement is carried out twice and the results are averaged using the setup described in Section II. Although the system was capable of applying up to 70 MPa stress on the standard sample, the applied stress was limited to 50 MPa to avoid buckling.

IV. Conclusion

A frequency-dependent magneto-elastic hysteresis model is proposed in this article. In this model, the anhysteretic magnetization formulated from the MS approach is used in the JA model. The effect of stress on magnetic properties is modeled in terms of anhysteretic magnetization while the hysteresis effect is included by using the JA model. The kink and crossing points are modeled using a Gaussian function. Kink, the localized widening of the hysteresis loop, is modeled by modifying the pinning parameter as a function of B. Dynamic losses are integrated into the proposed formalism by using the field separation approach. Among the two dynamic loss components, mechanical stress affects only the excess loss component. The stress effects on the excess loss component are incorporated in its coefficient using an exponential function. The model is applied to simulate dynamic hysteresis loops up to a frequency range of 1 kHz under uniaxial compressive and tensile stresses up to 50 MPa. The calculated losses using the proposed approach are in good agreement with the measured losses. The model offers an easy numerical implementation for a wide range of frequencies. It is demonstrated in this article through simulations of an SST device. The extension of this approach is to incorporate multiaxiality of stress in the model.

Acknowledgment

The authors thank the Coctel project coordinated by Renault-SAS, Guyancourt, France, and financed by Agence de l'Environnement et de la Maîtrise de l'Energie (ADEME). They would like to thank the Indian National Academy of Engineering (INAE) for support under INAE Chair Professorship Scheme and IIT Bombay for IRCC Research Award Grant. The authors would also like to thank the Critical Materials Institute (CMI) for partial support and collaboration.

References

[1] L. Bernard and L. Daniel, "Effect of stress on magnetic hysteresis losses in a switched reluctance motor: Application to stator and rotor shrink fitting," *IEEE Trans. Magn.*, vol. 51, no. 9, Sep. 2015, Art. no. 7002513.

[2] A. J. Moses, "Effects of stresses on magnetic properties of silicon-iron laminations," *J. Mater. Sci.*, vol. 9, no. 2, pp. 217–222, 1974.

[3] P. Baudouin, A. Belhadj, F. Breaban, A. Deffontaine, and Y. Houbaert, "Effects of laser and mechanical cutting modes on the magnetic properties of low and medium Si content nonoriented electrical steels," *IEEE Trans. Magn.*, vol. 38, no. 5, pp. 3213–3215, Sep. 2002.

[4] A. P. S. Baghel, J. B. Blumenfeld, L. Santandrea, G. Krebs, and L. Daniel, "Effect of mechanical stress on different core loss components along orthogonal directions in electrical steels," *Elect. Eng.*, vol. 101, pp. 845–853, Sep. 2019.

[5] A. P. S. Baghel *et al.*, "An alternative approach to model mechanical stress effects on magnetic hysteresis in electrical steels using complex permeability," *Comput. Mater. Sci.*, vol. 166, pp. 96–104, Aug. 2019.

[6] T. Suzuki and E. Matsumoto, "Comparison of Jiles–Atherton and Preisach models extended to stress dependence in magnetoelastic behaviors of a ferromagnetic material," *J. Mater. Process. Technol.*, vol. 161, pp. 141–145, Apr. 2005.

[7] L. Daniel, M. Rekik, and O. Hubert, "A multiscale model for magneto-elastic behaviour including hysteresis effects," *Arch. Appl. Mech.*, vol. 84, nos. 9–11, pp. 1307–1323, Oct. 2014.

[8] U. Aydin *et al.*, "Magneto-mechanical modeling of electrical steel sheets," *J. Magn. Magn. Mater.*, vol. 439, pp. 82–90, Oct. 2017.

[9] P. Rasilo *et al.*, "Flexible identification procedure for thermodynamic constitutive models for magnetostrictive materials," *Proc. Roy. Soc. A*, vol. 475, no. 2223, 2019, Art. no. 20180280.

[10] D. J. Craik and M. J. Wood, "Magnetization changes induced by stress in a constant applied field," *J. Phys. D, Appl. Phys.*, vol. 3, no. 7, pp. 1009–1016, 1970.

[11] R. Birss, "Magnetomechanical effects in the Rayleigh region," *IEEE Trans. Magn.*, vol. 7, no. 1, pp. 113–133, Mar. 1971.

[12] R. M. Bozorth, *Ferromagnetism*. New York, NY, USA: Van Nostrand, 1951.

[13] C. S. Schneider, "Effect of stress on the shape of ferromagnetic hysteresis loops," *J. Appl. Phys.*, vol. 97, no. 10, 2005, Art. no. 10E503.

[14] O. Perevertov and R. Schäfer, "Influence of applied tensile stress on the hysteresis curve and magnetic domain structure of grain-oriented Fe–3%Si steel," *J. Phys. D, Appl. Phys.*, vol. 47, no. 18, 2014, Art. no. 185001.

[15] O. Perevertov, "Influence of the applied elastic tensile and compressive stress on the hysteresis curves of Fe-3%Si non-oriented steel," *J. Magn. Mag. Mat.*, vol. 428, pp. 223–228, Apr. 2017.

[16] M. J. Sablik and D. C. Jiles, "Coupled magnetoelastic theory of magnetic and magnetostrictive hysteresis," *IEEE Trans. Magn.*, vol. 29, no. 4, pp. 2113–2123, Jul. 1993.

[17] H. ElBidweihy, E. Della Torre, Y. Jin, L. H. Bennett, and M. Ghahremani, "A Preisach-type magnetostriction model for materials exhibiting Villari reversal," *IEEE Trans. Magn.*, vol. 48, no. 11, pp. 3360–3362, Nov. 2012.

[18] B. S. Ram, A. P. S. Baghel, S. V. Kulkarni, K. Chwastek, and L. Daniel, "A hybrid product-multi-scale model for magneto-elastic behavior of soft magnetic materials," *Phys. B, Condens. Matter.*, vol. 571, pp. 301–306, Oct. 2019.

[19] H. Hauser, "Energetic model of ferromagnetic hysteresis: Isotropic magnetization," *J. Appl. Phys.*, vol. 96, no. 5, pp. 2753–2767, 2004.

[20] G. Bertotti, *Hysteresis in Magnetism*. San Diego, CA, USA: Academic, 1988.

[21] V. Permiakov, L. Dupré, A. Pulnikov, and J. Melkebeek, "Loss separation and parameters for hysteresis modelling under compressive and tensile stresses," *J. Magn. Magn. Mater.*, vols. 272–276, pp. 553–554, May 2004.

[22] L. Daniel, "An analytical model for the effect of multiaxial stress on the magnetic susceptibility of ferromagnetic materials," *IEEE Trans. Magn.*, vol. 49, no. 5, pp. 2037–2040, May 2013.

[23] D. Singh, F. Martin, P. Rasilo, and A. Belachen, "Magnetomechanical model for hysteresis in electrical steel sheet," *IEEE Trans. Magn.*, vol. 52, no. 11, Nov. 2016, Art. no. 7301109.

[24] A. P. S. Baghel and S. V. Kulkarni, "Dynamic loss inclusion in the Jiles–Atherton (JA) hysteresis model using the original JA approach and the field separation approach," *IEEE Trans. Magn.*, vol. 50, no. 2, Feb. 2014, Art. no. 7009004.

[25] L. Daniel and O. Hubert, "Equivalent stress criteria for the effect of stress on magnetic behavior," *IEEE Trans. Magn.*, vol. 46, no. 8, pp. 3089–3092, Aug. 2010.

[26] A. P. S. Baghel and S. V. Kulkarni, "Parameter identification of the Jiles–Atherton hysteresis model using a hybrid technique," *IET Electr. Power Appl.*, vol. 6, no. 9, pp. 689–695, Nov. 2012.

[27] S. V. Kulkarni and S. A. Khaparde, *Transformer Engineering: Design, Technology, and Diagnostics*. Boca Raton, FL, USA: CRC, 2012.

[28] E. Dlala, A. Belahcen, and A. Arkkio, "A fast fixed-point method for solving magnetic field problems in media of hysteresis," *IEEE Trans. Magn.*, vol. 44, no. 6, pp. 1214–1217, Jun. 2008.